The RORγt$^+$ subset of NKT cells displays unique sensitivity to cytokines

Kylie E. Webster[1,2*], Hee-Ok Kim[1], Konstantinos Kyparissoudis[3], Theresa M. Corpuz[1], Gabriela V. Pinget[1], Robert Brink[1,2], Gabrielle T. Belz[4,5], Jae-Ho Cho[1,2], Dale I. Godfrey[3] and Jonathan Sprent[1,2,6].

Affiliations:

1) Immunology Division, Garvan Institute of Medical Research, 384 Victoria Street, Darlinghurst, NSW 2010, Australia
2) St. Vincent's Clinical School, University of New South Wales, Sydney, NSW 2010, Australia.
3) Department of Microbiology and Immunology, University of Melbourne, Parkville, VIC 3010, Australia.
4) Molecular Immunology, The Walter and Eliza Hall Institute of Medical Research, 1G Royal Parade, Parkville, VIC 3052, Australia.
5) Department of Medical Biology, University of Melbourne, Parkville, VIC 3010, Australia.
6) WCU-IBB Program, POSTECH, Pohang, Korea

* To whom correspondence should be addressed.

E-mail: k.webster@garvan.org.au

Ph: +61 2 9295-8411

Fax: +61 2 9295-8404

Running Title: *Cytokine sensitivity of RORγt$^+$ NKT cells*

33911 Characters (excluding Materials and Methods and References); Figures: 5; Supplementary Figures: 5; References: 32.

Abstract

Natural killer T cells are innate-like T cells that rapidly recognise pathogens and produce cytokines that can shape the ensuing immune response. Recently, IL-17-producing NKT cells have been identified in mice and humans. Studies show that these RORγt-expressing cells have divergent developmental pathways and functional requirements from other NKT cells, yet the factors that maintain this population in the periphery have not been elucidated. Here we show that NKT17 cells also diverge in their survival requirements. In contrast to conventional NKT cells that are maintained by IL-15, RORγt$^+$ NKT cells are IL-15 independent and instead rely completely on IL-7. IL-7 initiates a TCR-independent expansion of NKT17 cells, thus supporting their homeostasis. Without IL-7, survival is dramatically impaired, yet residual cells remain lineage committed with no downregulation of RORγt evident. Their preferential response to IL-7 does not reflect enhanced signaling through STAT proteins, but instead is modulated via the PI3K/AKT/mTOR signaling pathway. The ability to compete for IL-7 correlates with lower SOCS3 levels and high density IL-7 receptor which is greater than most other T lymphocytes. This dependence on IL-7 is also reported for RORγt$^+$ innate lymphoid cells and CD4$^+$ Th17 cells, and suggests common survival requirements for functionally similar cells.

Introduction

Natural killer T (NKT) cells are lipid antigen-reactive, CD1d-restricted T cells that represent a critical element of the immune repertoire. They respond swiftly to pathogens, either by direct recognition of bacterial glycolipid antigen (Kinjo et al., 2011) or indirectly via cytokine and self-lipid antigen ligation (Brigl et al., 2011; Zeissig et al., 2012) and rapidly produce a range of cytokines that can dictate the course of the subsequent immune response.

Recently it was observed that NKT cells produce IL-17, a cytokine crucial for host defence against bacterial and fungal infections (Coquet et al., 2008; Michel et al., 2007; Moreira-Teixeira et al., 2011; Rachitskaya et al., 2008). These NKT17 cells constitutively express the transcription factor retinoic acid receptor-related orphan receptor γt (RORγt), are NK1.1 negative, and respond to IL-1β and IL-23 by upregulating IL-17 (Doisne et al., 2009; Doisne et al., 2011; Rachitskaya et al., 2008). NKT17 cells are positioned in 'gateway' tissues such as skin, lung and peripheral lymph nodes (pLN), with lower proportions in the spleen and liver (Doisne et al., 2009; Michel et al., 2007), making them well-placed to respond early to a pathogenic insult.

That IL-17 is of clinical importance in infection and autoimmunity is now clear (Korn et al., 2009), and a role for NKT17 cells in this response is emerging. NKT cells can make IL-17 in response to *Streptococcus pneumonia* and *Klebsiella pneumoniae*, causes of community-acquired and nosocomial pneumonia (Kinjo et al., 2011; Price et al., 2012). Additionally, ozone, a component of air pollution, induces an airway hyperreactivity that requires IL-17 and NKT cells (Pichavant et al., 2008). Furthermore, in the mouse model of multiple sclerosis, NKT cells produce a significant proportion of the early IL-17, along with other innate-like T cells (Price et al., 2012).

NKT17 cells acquire RORγt expression in the thymus (Michel et al., 2008), where their developmental decisions are mediated by low expression of Th-POK and SMAD4-dependent TGFβ

signaling (Enders et al., 2012; Engel et al., 2012; Havenar-Daughton et al., 2012). That NKT17 cells follow distinct developmental pathways raises questions about their ensuing maintenance. Homeostasis of NKT cells was found to require IL-15, however NKT17 cells had yet to be identified at this time (Matsuda et al., 2002; Ranson et al., 2003). In the first study to examine pLN NKT cells, it was found that IL-15Rβ expression was very low on NK1.1$^-$ cells (Doisne et al., 2009). This was later shown to also be the case for thymic RORγt$^+$ NKT cells (Havenar-Daughton et al., 2012) and splenic IL-17RB$^+$ NKT cells (of which RORγt$^+$ are a subset) (Watarai et al., 2012). Interestingly, in mice with a mutant form of IL-15, the IL-17RB$^-$ cells are the most significantly decreased (Watarai et al., 2012). These observations strongly suggest that RORγt$^+$ NKT17 cells don't share the same level of dependency on IL-15 as other NKT cells. Consequently, the factors that maintain this population in the periphery are unknown.

Here we show that, in contrast to the bulk of NKT cells, the homeostasis of IL-17-producing RORγt$^+$ NKT cells depends on IL-7 rather than IL-15. The rapid proliferation of RORγt$^+$ NKT cells to IL-7 requires activation of the PI3K/AKT/mTOR signaling pathway and is precisely tuned to the density of cell surface IL-7Rα, which is expressed at much higher levels on these NKT cells compared to most other T cell types. These survival requirements indicate that RORγt$^+$ NKT17 cells share a resource niche with differentiated CD4$^+$ Th17 cells and RORγt$^+$ innate lymphoid cells (ILCs), and suggest IL-7R antagonism as a potential treatment for IL-17-driven pathology.

Results and Discussion

IL-15 has no role in RORγt$^+$ NKT cell homeostasis

To investigate the role of IL-15 in homeostasis of NKT17 cells, we first analysed the expression of the IL-15R/IL-2R β chain, CD122, on NKT cell subsets as delineated by CD4 and NK1.1 (Fig. 1 A) and RORγt (Fig. 1 B). In agreement with previous findings (Doisne et al., 2009; Havenar-Daughton

et al., 2012; Watarai et al., 2012), we observed that NKT17 cells, contained within the $CD4^{-}NK1.1^{-}$ subset or directly analysed by RORγt, had minimal expression of CD122, suggesting decreased sensitivity to IL-15.

To more directly assess the relevance of IL-15 for maintenance of NKT17 cells, we then analysed IL-15-deficient mice. Although total NKT cell numbers are considerably reduced in the absence of IL-15 (Matsuda et al., 2002), these mice showed a significant increase in the proportion of IL-17-producing (Fig. 1 C) and also $ROR\gamma t^{+}$ NKT cells (Fig. 1 D). Importantly however, total numbers of $ROR\gamma t^{+}$ cells were unchanged in IL-15-deficient mice, indicating that the dependence of NKT cells on IL-15 applied selectively to RORγt-negative cells (Fig. 1 D).

To further evaluate the role of IL-15, we examined lymphopenia-driven proliferation of NKT cells in IL-15-deficient hosts. Purified NKT cells were CFSE labelled and adoptively transferred into sub-lethally irradiated control or $IL\text{-}15^{-/-}$ animals. For the $ROR\gamma t^{-}$ subset, proliferation of these cells was limited, typical of slow homeostatic proliferation, and was reduced in $IL\text{-}15^{-/-}$ mice (Fig. 1 E), thereby confirming prior findings with unseparated NKT cells (Matsuda et al., 2002). In marked contrast, proliferation of the $ROR\gamma t^{+}$ subset was rapid and as prominent in $IL\text{-}15^{-/-}$ as in WT hosts. These data indicate that, for lymphopenia-induced proliferation of NKT cells, IL-15 signaling is important only for $ROR\gamma t^{-}$ and not for $ROR\gamma t^{+}$ cells.

Preferential expansion of IL-17-producing NKT cells after *in vivo* IL-7 treatment

IL-7, another common homeostatic cytokine, is reported to play either no role (Ranson et al., 2003) or a minor role (Matsuda et al., 2002) in NKT cell homeostasis. Since $ROR\gamma t^{+}$ NKT cells were not considered in these studies, we re-examined the response of NKT cells to IL-7. Firstly, we injected mice with exogenous IL-7 in the form of cytokine/antibody complexes (Boyman et al., 2008); control mice received complexes of IL-2/IL-2 mAb. After three daily injections, cytokine

production by purified NKT cells was assessed *ex vivo*. IL-2-expanded NKT cells showed enhanced production of a variety of Th1 and Th2 cytokines, but interestingly less IL-17. In stark contrast, for IL-7-expanded NKT cells, only IL-17 was significantly elevated (Fig. 2 A). Likewise, intracellular cytokine staining showed that IL-7-expanded NKT cells displayed enhanced synthesis of IL-17 (Fig. 2 B).

This finding raised the question whether IL-7 signaling specifically stimulated IL-17 production or, alternatively, caused selective expansion of IL-17-producing cells. Examining this question showed that IL-7 injection did indeed caused a selective expansion of RORγt^{+} NKT cells in spleen, liver and pLN (Fig. 2 C, Fig. S1). While RORγt^{+} NKT cells are CD4 positive and negative, both of which can make IL-17, it was the CD4 negative fraction that preferentially responded to IL-7 (Fig. S2). The preferential expansion to IL-7 was highly specific, as it could not be replicated with either IL-2 or IL-15 injections, with both but particularly IL-15, favouring the RORγt^{-} subset (Fig. 2 D).

RORγt^{+} NKT cells cannot proliferate or survive in the absence of IL-7

Injection of exogenous IL-7 showed that this cytokine specifically targets RORγt^{+} NKT cells for expansion. Likewise, RORγt^{+} NKT cells rapidly proliferate in lymphopenic hosts (an environment with elevated IL-7) as demonstrated in Figure 1E. As such, we questioned whether IL-7 is the cytokine responsible for the normal homeostasis and survival of these cells.

Genetic deletion of IL-7 renders mice severely lymphopenic, due to its broad role in lymphopoiesis and T cell survival (von Freeden-Jeffry et al., 1995). However, IL-7$^{-/-}$ mice do have peripheral NKT cells, albeit in reduced numbers (Matsuda et al., 2002). Significantly, we found that the residual NKT cells in IL-7$^{-/-}$ mice were totally unable to synthesize IL-17, and instead were biased to synthesis of IFNγ (Fig. 3 A). This suggests that either IL-7 offers NKT17 cells a functional advantage, or it is involved in their survival. Indeed we found that IL-7$^{-/-}$ mice have a profound and

selective reduction in RORγt$^+$ NKT cells, being barely detectable by flow cytometry in the spleen, liver and thymus (Fig. 3 B,C). Collectively, these findings indicate that IL-7 is obligatory for the development of the IL-17-producing RORγt$^+$ subset of NKT cells.

The above experiments did not reveal whether IL-7 influences the survival of mature RORγt$^+$ NKT cells. To investigate this question, purified NKT cells were adoptively transferred into sub-lethally irradiated control or IL-7$^{-/-}$ animals to examine lymphopenia-induced proliferation. For the RORγt$^-$ subset, proliferation was similar in IL-7$^{-/-}$ and control recipients, although recovery was reduced (Fig. 3 D). In marked contrast, an IL-7-deficient environment was clearly prohibitive for the RORγt$^+$ subset and led to reduced proliferation and negligible total recovery of the injected cells (Fig. 3 D). Hence, as for initial cell formation, the survival and homeostasis of mature RORγt$^+$ NKT cells was critically dependent on contact with IL-7; contact with IL-15 was irrelevant (compare Fig. 1 E with 3 D, which were part of the same experiment).

Strong IL-7-driven expansion of RORγt$^+$ NKT cells is TCR independent and does not reflect enhanced signaling through STAT5 or STAT3

Like memory T cells, NKT cell homeostasis is reported to be independent of TCR signaling (Matsuda et al., 2002). We found that this also applied to the RORγt$^+$ subset (Fig. 4 A). Stimulation of transferred CFSE-labelled NKT cells with IL-7/IL-7 mAb resulted in rapid proliferation of the RORγt$^+$ subset, regardless of the host environment being control B6 or deficient in CD1d.

Since IL-7 signaling occurs through the Jak/STAT pathway and involves phosphorylation of STAT5 (Carrette and Surh, 2012) and STAT3 (Michel et al., 2012), the high sensitivity of RORγt$^+$ NKT cells to IL-7 might reflect enhanced STAT phosphorylation. However, exposure to titrated concentrations of IL-7 *in vitro* showed that STAT5 was rapidly phosphorylated in both RORγt$^+$ and RORγt$^-$ NKT cells to an equivalent degree (Fig. 4 B, Fig. S3). Likewise, both subsets showed

equivalent sensitivity to STAT3 activation (Fig. 4 B). These data imply that a preferential activation of the Jak/STAT pathway is not the mechanism by which IL-7 exerts its superior effects on RORγt$^+$ NKT cells.

IL-7-mediated RORγt$^+$ NKT cell expansion requires activation of the PI3K/Akt/mTOR pathway

In T cells, the phosphoinositide 3-kinase (PI3K) pathway is activated after engagement of TCR and costimulatory receptors (Deane and Fruman, 2004). Activation after IL-7 signaling alone is much slower in onset (hours rather than minutes), but is necessary for cell cycle entry (Lali et al., 2004). We examined PI3K-dependent signaling in purified NKT cells after overnight culture with IL-7. Notably, IL-7 led to far higher phosphorylation of AKT in the RORγt$^+$ subset, without the need for TCR-CD1d interactions (Fig. 4 C). Further studies showed that IL-7-induced proliferation of RORγt$^+$ cells was blocked by the PI3K inhibitor, LY294002, and also by the mTOR inhibitor, rapamycin, (Fig. 4 D). These findings indicate that the strong IL-7-induced proliferation of RORγt$^+$ NKT cells is crucially dependent on the PI3K/Akt/mTOR signaling pathway.

SOCS proteins are lower in RORγt$^+$ compared to RORγt$^-$ NKT cells

Since T cell sensitivity to IL-7 has been associated with lower levels of SOCS1 and SOCS3 proteins (Liu et al., 2010; Pellegrini et al., 2011), we asked whether the strong reactivity of RORγt$^+$ NKT cells to IL-7 might reflect altered levels of these molecules. Indeed, intracellular staining showed that, compared to RORγt$^-$ NKT cells, the RORγt$^+$ subset had significantly reduced levels of SOCS3, and also SOCS1, but to a lesser extent (Fig. 5 A). Furthermore, for sorted NK1.1$^-$ CCR6$^+$CD103$^+$ and NK1.1$^+$CCR6$^-$CD103$^-$ subsets (representative of RORγt$^+$ and RORγt$^-$ cells, respectively) (Fig. S4) (Doisne et al., 2009), the expression of the *Socs3* gene was clearly lower in RORγt$^+$ NKT cells (Fig. 5B). Collectively, these data show that hyper-responsiveness to IL-7 correlates with a lower intrinsic expression of SOCS3.

High IL-7Rα expression is crucial for the strong proliferative response of RORγt$^+$ NKT cells

Since IL-7 is a limited resource, an enhanced capacity to bind this cytokine would offer a distinct advantage. Indeed we found that IL-7Rα expression is higher on RORγt$^+$ than RORγt$^-$ NKT cells (Fig. 5 C, Fig. S5). IL-7Rα expression on RORγt$^+$ NKT cells was also much higher than on conventional T cells, eg CD8$^+$ T cells (Fig. 5 D), and correlated with the conspicuous proliferative response of RORγt$^+$ cells to IL-7 (Fig. 5 E).

The density of IL-7Rα varies greatly amongst RORγt-negative cells. With this in mind, we sorted pooled spleen and pLN into populations with low and intermediate-high expression of IL-7Rα (Fig. S4) to directly test the effect of receptor density. Significantly, IL-7 induced stronger proliferation of IL-7Rα$^{INT-HIGH}$ than IL-7Rα^{LOW} cells (Fig. 5 F). Hence, both for RORγt$^+$ and RORγt$^-$ cells, proliferative responses of NKT subsets to IL-7 correlated directly with surface levels of IL-7R.

IL-7 alone does not induce or stabilize RORγt expression in peripheral NKT17 cells

Despite not being dependent on IL-7 for homeostasis, the moderate proliferation of RORγt$^-$ NKT cells to IL-7 poses the question of whether RORγt$^+$ NKT cells are indeed a stable, separate lineage. One study showed that RORγt$^-$ NKT cells can be induced to make IL-17 in vitro (Monteiro et al., 2013), while experiments with ILCs suggest that IL-7 may stabilize their RORγt expression (Vonarbourg et al., 2010). In light of this, we questioned whether IL-7 is important for the stable expression of RORγt in NKT cells, and whether constant IL-7 or deprivation of this signal could induce a switch in RORγt expression. RORγt-negative NKT cells were purified from RORγt-GFP mice (Eberl et al., 2004), labelled with Cell Trace Violet (CTV), and transferred into congenic B6 mice (Fig. S4). Following five days of IL-7/IL-7 mAb treatment, cells again displayed moderate

proliferation, but GFP was only detected in an average of 0.5% of donor cells (Fig. 5 G), indicating that even high dose IL-7 was unlikely to induce conversion to RORγt.

When purified RORγt^{+} cells were transferred into sublethally irradiated IL-7$^{-/-}$ hosts, cell survival was poor, at only a fraction of that recovered from IL-7 replete mice (Fig. 5 H). Interestingly, surviving donor cells retained their RORγt expression. As such, a strong IL-7 signal alone cannot induce RORγt expression, and neither can the cells 'revert' to a RORγt-negative state to survive in the absence of IL-7. These data support the concept that RORγt-expressing NKT17 cells are a defined lineage, with distinct requirements for survival.

In summary, our data demonstrate that IL-7 stimulation can initiate TCR-independent expansion of RORγt^{+} NKT17 cells, and thus support their homeostasis. Their absolute requirement for IL-7 and indifference to IL-15, means that these cells are not in competition for resources with the majority of NKT cells. Instead, the dependence on IL-7 reveals a shared characteristic with other IL-17-producing cells, as it has been recently found that differentiated Th17 cells (Liu et al., 2010), RORγt^{+} innate lymphoid cells (ILCs) (Satoh-Takayama et al., 2010) and IL-17-producing γδ T cells (Michel et al., 2012) utilize IL-7 for their survival. As such, the NKT17 niche appears to be shaped, not by other NKT cells, but by cells with similar functional properties.

Materials & Methods

Mice

C57BL/6 (B6) and B6.Ly5.1 mice were obtained from the Animal Resources Centre (Perth, Australia). IL-$7^{-/-}$ and IL-$15^{-/-}$ colonies were maintained at the Australian Bioresources Centre (Mossvale, Australia) and Rorc(γt)^{GFP} mice were maintained at The Walter and Eliza Hall Institute (Melbourne, Australia). All mice were used at the age of 6-12 wk. Animals were housed under conventional barrier protection and handled in accordance with the Garvan Institute of Medical Research and St Vincent's Hospital Animal Experimentation and Ethics Committee, which comply with the Australian code of practice for the care and use of animals for scientific purposes.

Flow cytometry and antibodies

Cell suspensions of spleen and lymph nodes were prepared according to standard protocols. Lymphocytes from single cell suspensions of perfused livers were separated by a 33% isotonic Percoll density gradient (GE Healthcare). Cell suspensions were stained for FACS analysis using the following antibodies (obtained from eBioscience unless otherwise stated): FITC- anti-CD4 (RM4-5, BD Biosciences), anti-NK1.1 (PK136), anti-CD122 (TM-β1, BD Biosciences) and anti-CD127 (A7R34); Alexa Fluor 488-anti-phosphorylated-STAT5 (47/Stat5 (pY694), BD Biosciences), anti-phosphorylated-STAT3 (4/P-STAT3 (pY705), BD Biosciences), and anti-phosphorylated-AKT (Ser473, D9E, Cell Signaling); PE- anti-CD4 (RM4-5, BD Biosciences), anti-RORγ(t) (B2D), and anti-IFNγ (XMG1.2); PerCP-Cy5.5- anti-CD4 (RM4-5); biotinylated- anti-CD122 (TM-β1, BD Biosciences); APC-anti-TCR β (H57-597), anti-CD127 (A7R34) and anti-IL-17A (eBio17B7); Pacific Blue-anti-TCR β (H57-597, Biolegend), anti-IL-17A (TC11-18H10.1, Biolegend) and anti-IFNγ (XMG1.2) and Pacific Blue streptavidin (Molecular Probes); and Rat IgG2a and Rat IgG2b Isotype Control FITC, biotin, and APC; and Rabbit Isotype Control Alexa Fluor-488 (Cell Signaling). PE- or Brilliant Violet 421-conjugated mouse CD1d tetramer loaded with α-GalCer (purchased from Sapphire biosciences or kindly provided by Prof. Paul Savage,

Brigham Young University, UT, USA) was produced in-house as previously described (Matsuda et al., 2000), using recombinant baculovirus encoding histamine-tagged mouse CD1d and mouse β2-microglobulin, originally provided by Prof. Mitchell Kronenberg (La Jolla Institute for Allergy and Immunology, CA USA). For detection of p-STAT5 and p-STAT3, single cell suspensions were surface stained with Abs against TCRβ and αGC/CD1d tetramer for 15 min, then stimulated with either mIL-7 (10 ng/ml unless otherwise indicated) for 10 min at 37°C. The cells were then immediately fixed, permeabilized and stained with pSTAT-5 and RORγt, or p-STAT3 and RORγt according to the manufacturer's instructions. For detection of p-AKT, sorted NKT cells were stimulated overnight with 10 ng/ml mIL-7, then fixed, permeabilized and stained with pAKT and RORγt according to the manufacturer's instructions. To detect SOCS1 and SOCS3, fixed and permeabilized cells were stained with rabbit polyclonal anti-SOCS1 (ab3691) and SOCS3 (ab16030) (Abcam), followed by anti-rabbit FITC. Samples were analyzed on a CantoII or sorted using a FACSAria (BD Biosciences). Data were analyzed using FloJo software (Treestar, Inc).

Injection of cytokine / mAb complexes

To make cytokine/mAb complexes, recombinant mouse IL-2, IL-7 or IL-15 (Peprotech) were mixed with anti-IL-2 (clone JES6-1, eBioscience; clone S4B6, BD Biosciences) or anti-IL-7 mAb (clone M25, Bio X Cell) or IL-15 Rα/Fc Chimera (R&D Systems) and incubated at 37°C for 30 min. Mice were injected i.p. with a dose of 1 μg cytokine + 5 μg mAb on three consecutive days.

Cytokine measurement

For cytokine analysis from cell culture supernatant, all cytokines were assayed by using BD Biosciences cytometric bead array flex set for mice (IL-2, IL-3, IL-4, IL-5, IL-6, IL-9, IL-10, IL-12p70, IL-13, IFN-γ, TNFα, GMCSF, and IL-17A). NKT cells were purified by cell sorting from pooled spleens treated with PBS, IL-2/JES6-1 or IL-7/M25. Cells were cultured in RPMI-1640 supplemented with 10% fetal calf serum, 10 mM HEPES, 1 mM Na pyruvate, 50 U/ml penicillin,

50 μg/ml streptomycin, 2 mM L-glutamine, 55 μm β-mercaptoethanol in 96-well plates coated with anti-CD3 Ab (clone 145-2C11) and anti-CD28 (clone 37.51) at a concentration of 10 μg/ml. Culture supernatants were analyzed at 24 and 72h. For intracellular cytokine staining, cells were incubated at 37°C in complete RPMI-1640 medium with PMA (10 ng/ml) and ionomycin (1 μg/ml) for 4 h with monensin in 24-well plates at a concentration of 6 x 10^6 cells/ml. Surface staining was performed with fluorescently labeled antibodies, after which cells were resuspended in Fixation/Permeabilization solution (BD Cytofix/Cytoperm kit, BD Biosciences), and intracellular staining performed as per the manufacturer's protocol.

Isolation of NKT cells

Single cell suspensions of spleen, peripheral lymph nodes or liver, were first negatively depleted by staining with anti-B220-biotin and anti-CD8-biotin followed by incubation with Dynabeads Biotin Binder (Invitrogen) and magnetic separation. The depleted fraction was stained with anti-TCR β-APC and anti-α-GalCer/CD1d tetramer-Brilliant Violet 421 (NKT cells). In some cases, cells were also stained with CD127 and CD122 to isolate cells with equivalent CD127 density, or CD103, CCR6 and NK1.1 to isolate cells representative of RORγt-positive and negative subsets as indicated. GFP was used to isolate RORγt-expressing cells from Rorc(γt)^{GFP} mice. Cell sorting was performed on a FACSAria (BD Biosciences) to obtain a pure population of NKT cells.

CFSE and CTV labeling

Lymphocytes were washed once in 0.1% BSA in PBS, and labeled with 5 μM (in vivo analysis) or 2.5 μM (in vitro analysis) CFSE (Molecular Probes), or 10 μM CTV (Molecular Probes) at a density of 1 x 10^7 cells/ml 0.1% BSA in PBS for 10 min at 37°C (CFSE) or 20 min at room temperature (CTV) in the dark. The reaction was stopped with RPMI 10% FCS and washed twice.

Adoptive cell transfers

Congenic Ly5.1^{+} NKT cells were purified by cell sorting, labeled with CFSE, and injected intravenously into C57BL/6, IL-15$^{-/-}$ or IL-7$^{-/-}$ recipient mice sublethally irradiated (550 RAD) one day before cell transfer, or non-irradiated C57BL/6 or CD1d$^{-/-}$ recipients. For analysis of homeostatic expansion, spleens and livers were harvested on day 7 and the Ly5.1^{+} donor cells quantified using flow cytometry. For analysis of CD1d dependence, mice were injected with IL-7/IL-7 mAb (1 μg/ 5 μg) on days 1, 2, 3, and anti-CD1d (50 μg) or Rat IgG2b isotype control (50 μg) on days 1 and 3 (for CD1d$^{-/-}$ and C57BL/6 respectively). Livers were harvested on day 7 and Ly5.1^{+} donor cells quantified using flow cytometry.

In vitro proliferation assay

NKT cells were purified from spleen and lymph nodes by cell sorting, CFSE labeled and cultured in 96-well plates (5 x 10^4 cells/well) for 72 h with IL-7 (10 ng/ml). In some cases, cells were pre-incubated with specific inhibitors for 1 h before the addition of IL-7; LY294002 (5, 10, 15 μm; Calbiochem) and Rapamycin (25 nm; Merck). After culture, cells were stained with RORγt antibody, and analyzed by flow cytometry.

Real-time PCR

RNA was isolated from sorted NKT cell subsets representative of RORγt^{+} and RORγt^{-} cells, pLN NK1.1^{-}CCR6^{+}CD103^{+} cells and splenic or pLN NK1.1^{+}CCR6^{-}CD103^{-} cells, using Qiagen RNeasy Micro or Mini kits as per the manufacturer's instructions. RNA was reverse transcribed into cDNA using the Qiagen QuantiTect Reverse Transcription kit. Real-time PCR for the detection of *Socs1* mRNA and *Socs3* mRNA was performed using TaqMan gene expression assays (Mm00782550_s1*) and (Mm00545913_s1*) (Applied Biosystems). Gapdh mRNA was used as an endogenous control. Samples were assayed on an ABI 7900 HT Real-Time PCR machine.

Statistical analysis

Results are presented as means ± SEM. In most cases, statistical significance was assessed using the unpaired, two-tailed Student's t test, performed in Prism software (Graphpad). In the case of non-Gaussian distribution, the Mann Whitney test was used for data analysis, while for samples with unequal variance the Welch correction was applied. Bonferroni correction was used to adjust p-values when performing multiple comparisons in Figure 2a (adjusted for two hypotheses). Paired t-tests were used to compare the MFI of RORγt^{+} and RORγt^{-} subsets. Numbers of mice and experiments are detailed in Figure Legends.

Acknowledgements

The authors thank the Biological Testing Facility (Garvan Institute) for animal breeding. We thank Robert Salomon and David Snowden for cell sorting, Amanda Hong for genotyping and Marcin Ciula for CD1d tetramer preparation. This work was supported by National Health and Medical Research Council (NHMRC) Australia grants 1045647 (K.E.W), 1011388 (J-H.C), 454569/1013667 (D.I.G), 1016953 (J.S) and fellowships 1020770 (D.I.G), 596805 (J.S). JS is a co-founder in a company for developing the therapeutic use of cytokine/mAb complexes. The authors have no other competing financial interests.

Abbreviations

IL – Interleukin

RORγt – retinoic acid receptor-related orphan receptor γt

NKT – natural killer T

pLN – peripheral lymph nodes

mAb – monoclonal antibody

WT – wild-type

SOCS – suppressor of cytokine signaling

MFI – mean fluorescence intensity

References

Boyman, O., C. Ramsey, D.M. Kim, J. Sprent, and C.D. Surh. 2008. IL-7/anti-IL-7 mAb complexes restore T cell development and induce homeostatic T Cell expansion without lymphopenia. *J. Immunol.* 180:7265-7275.

Brigl, M., R.V. Tatituri, G.F. Watts, V. Bhowruth, E.A. Leadbetter, N. Barton, N.R. Cohen, F.F. Hsu, G.S. Besra, and M.B. Brenner. 2011. Innate and cytokine-driven signals, rather than microbial antigens, dominate in natural killer T cell activation during microbial infection. *J. Exp. Med.* 208:1163-1177.

Carrette, F., and C.D. Surh. 2012. IL-7 signaling and CD127 receptor regulation in the control of T cell homeostasis. *Semin. Immunol.* 24:209-217.

Coquet, J.M., S. Chakravarti, K. Kyparissoudis, F.W. McNab, L.A. Pitt, B.S. McKenzie, S.P. Berzins, M.J. Smyth, and D.I. Godfrey. 2008. Diverse cytokine production by NKT cell subsets and identification of an IL-17-producing CD4-NK1.1- NKT cell population. *Proc. Natl. Acad. Sci. U. S. A.* 105:11287-11292.

Deane, J.A., and D.A. Fruman. 2004. Phosphoinositide 3-kinase: diverse roles in immune cell activation. *Annu. Rev. Immunol.* 22:563-598.

Doisne, J.M., C. Becourt, L. Amniai, N. Duarte, J.B. Le Luduec, G. Eberl, and K. Benlagha. 2009. Skin and peripheral lymph node invariant NKT cells are mainly retinoic acid receptor-related orphan receptor (gamma)t+ and respond preferentially under inflammatory conditions. *J. Immunol.* 183:2142-2149.

Doisne, J.M., V. Soulard, C. Becourt, L. Amniai, P. Henrot, C. Havenar-Daughton, C. Blanchet, L. Zitvogel, B. Ryffel, J.M. Cavaillon, J.C. Marie, I. Couillin, and K. Benlagha. 2011. Cutting edge: crucial role of IL-1 and IL-23 in the innate IL-17 response of peripheral lymph node NK1.1- invariant NKT cells to bacteria. *J. Immunol.* 186:662-666.

Eberl, G., S. Marmon, M.J. Sunshine, P.D. Rennert, Y. Choi, and D.R. Littman. 2004. An essential function for the nuclear receptor RORgamma(t) in the generation of fetal lymphoid tissue inducer cells. *Nature immunology* 5:64-73.

Enders, A., S. Stankovic, C. Teh, A.P. Uldrich, M. Yabas, T. Juelich, J.A. Altin, S. Frankenreiter, H. Bergmann, C.M. Roots, K. Kyparissoudis, C.C. Goodnow, and D.I. Godfrey. 2012. ZBTB7B (Th-POK) regulates the development of IL-17-producing CD1d-restricted mouse NKT cells. *J. Immunol.* 189:5240-5249.

Engel, I., M. Zhao, D. Kappes, I. Taniuchi, and M. Kronenberg. 2012. The transcription factor Th-POK negatively regulates Th17 differentiation in Valpha14i NKT cells. *Blood* 120:4524-4532.

Havenar-Daughton, C., S. Li, K. Benlagha, and J.C. Marie. 2012. Development and function of murine RORgammat+ iNKT cells are under TGF-beta signaling control. *Blood* 119:3486-3494.

Kinjo, Y., P. Illarionov, J.L. Vela, B. Pei, E. Girardi, X. Li, Y. Li, M. Imamura, Y. Kaneko, A. Okawara, Y. Miyazaki, A. Gomez-Velasco, P. Rogers, S. Dahesh, S. Uchiyama, A. Khurana, K. Kawahara, H. Yesilkaya, P.W. Andrew, C.H. Wong, K. Kawakami, V. Nizet, G.S. Besra, M. Tsuji, D.M. Zajonc, and M. Kronenberg. 2011. Invariant natural killer T cells recognize glycolipids from pathogenic Gram-positive bacteria. *Nature immunology* 12:966-974.

Korn, T., E. Bettelli, M. Oukka, and V.K. Kuchroo. 2009. IL-17 and Th17 Cells. *Annu. Rev. Immunol.* 27:485-517.

Lali, F.V., J. Crawley, D.A. McCulloch, and B.M. Foxwell. 2004. A late, prolonged activation of the phosphatidylinositol 3-kinase pathway is required for T cell proliferation. *J. Immunol.* 172:3527-3534.

Liu, X., S. Leung, C. Wang, Z. Tan, J. Wang, T.B. Guo, L. Fang, Y. Zhao, B. Wan, X. Qin, L. Lu, R. Li, H. Pan, M. Song, A. Liu, J. Hong, H. Lu, and J.Z. Zhang. 2010. Crucial role of

interleukin-7 in T helper type 17 survival and expansion in autoimmune disease. *Nat. Med.* 16:191-197.

Matsuda, J.L., L. Gapin, S. Sidobre, W.C. Kieper, J.T. Tan, R. Ceredig, C.D. Surh, and M. Kronenberg. 2002. Homeostasis of V alpha 14i NKT cells. *Nature immunology* 3:966-974.

Matsuda, J.L., O.V. Naidenko, L. Gapin, T. Nakayama, M. Taniguchi, C.R. Wang, Y. Koezuka, and M. Kronenberg. 2000. Tracking the response of natural killer T cells to a glycolipid antigen using CD1d tetramers. *J. Exp. Med.* 192:741-754.

Michel, M.L., A.C. Keller, C. Paget, M. Fujio, F. Trottein, P.B. Savage, C.H. Wong, E. Schneider, M. Dy, and M.C. Leite-de-Moraes. 2007. Identification of an IL-17-producing NK1.1(neg) iNKT cell population involved in airway neutrophilia. *J. Exp. Med.* 204:995-1001.

Michel, M.L., D. Mendes-da-Cruz, A.C. Keller, M. Lochner, E. Schneider, M. Dy, G. Eberl, and M.C. Leite-de-Moraes. 2008. Critical role of ROR-gammat in a new thymic pathway leading to IL-17-producing invariant NKT cell differentiation. *Proc. Natl. Acad. Sci. U. S. A.* 105:19845-19850.

Michel, M.L., D.J. Pang, S.F. Haque, A.J. Potocnik, D.J. Pennington, and A.C. Hayday. 2012. Interleukin 7 (IL-7) selectively promotes mouse and human IL-17-producing gammadelta cells. *Proc. Natl. Acad. Sci. U. S. A.* 109:17549-17554.

Monteiro, M., C.F. Almeida, A. Agua-Doce, and L. Graca. 2013. Induced IL-17-producing invariant NKT cells require activation in presence of TGF-beta and IL-1beta. *J. Immunol.* 190:805-811.

Moreira-Teixeira, L., M. Resende, M. Coffre, O. Devergne, J.P. Herbeuval, O. Hermine, E. Schneider, L. Rogge, F.M. Ruemmele, M. Dy, A. Cordeiro-da-Silva, and M.C. Leite-de-Moraes. 2011. Proinflammatory environment dictates the IL-17-producing capacity of human invariant NKT cells. *J. Immunol.* 186:5758-5765.

Pellegrini, M., T. Calzascia, J.G. Toe, S.P. Preston, A.E. Lin, A.R. Elford, A. Shahinian, P.A. Lang, K.S. Lang, M. Morre, B. Assouline, K. Lahl, T. Sparwasser, T.F. Tedder, J.H. Paik, R.A.

DePinho, S. Basta, P.S. Ohashi, and T.W. Mak. 2011. IL-7 engages multiple mechanisms to overcome chronic viral infection and limit organ pathology. *Cell* 144:601-613.

Pichavant, M., S. Goya, E.H. Meyer, R.A. Johnston, H.Y. Kim, P. Matangkasombut, M. Zhu, Y. Iwakura, P.B. Savage, R.H. DeKruyff, S.A. Shore, and D.T. Umetsu. 2008. Ozone exposure in a mouse model induces airway hyperreactivity that requires the presence of natural killer T cells and IL-17. *J. Exp. Med.* 205:385-393.

Price, A.E., R.L. Reinhardt, H.E. Liang, and R.M. Locksley. 2012. Marking and quantifying IL-17A-producing cells in vivo. *PloS one* 7:e39750.

Rachitskaya, A.V., A.M. Hansen, R. Horai, Z. Li, R. Villasmil, D. Luger, R.B. Nussenblatt, and R.R. Caspi. 2008. Cutting edge: NKT cells constitutively express IL-23 receptor and RORgammat and rapidly produce IL-17 upon receptor ligation in an IL-6-independent fashion. *J. Immunol.* 180:5167-5171.

Ranson, T., C.A. Vosshenrich, E. Corcuff, O. Richard, V. Laloux, A. Lehuen, and J.P. Di Santo. 2003. IL-15 availability conditions homeostasis of peripheral natural killer T cells. *Proc. Natl. Acad. Sci. U. S. A.* 100:2663-2668.

Satoh-Takayama, N., S. Lesjean-Pottier, P. Vieira, S. Sawa, G. Eberl, C.A. Vosshenrich, and J.P. Di Santo. 2010. IL-7 and IL-15 independently program the differentiation of intestinal CD3-NKp46+ cell subsets from Id2-dependent precursors. *J. Exp. Med.* 207:273-280.

von Freeden-Jeffry, U., P. Vieira, L.A. Lucian, T. McNeil, S.E. Burdach, and R. Murray. 1995. Lymphopenia in interleukin (IL)-7 gene-deleted mice identifies IL-7 as a nonredundant cytokine. *J. Exp. Med.* 181:1519-1526.

Vonarbourg, C., A. Mortha, V.L. Bui, P.P. Hernandez, E.A. Kiss, T. Hoyler, M. Flach, B. Bengsch, R. Thimme, C. Holscher, M. Honig, U. Pannicke, K. Schwarz, C.F. Ware, D. Finke, and A. Diefenbach. 2010. Regulated expression of nuclear receptor RORgammat confers distinct functional fates to NK cell receptor-expressing RORgammat(+) innate lymphocytes. *Immunity* 33:736-751.

Watarai, H., E. Sekine-Kondo, T. Shigeura, Y. Motomura, T. Yasuda, R. Satoh, H. Yoshida, M. Kubo, H. Kawamoto, H. Koseki, and M. Taniguchi. 2012. Development and function of invariant natural killer T cells producing T(h)2- and T(h)17-cytokines. *PLoS biology* 10:e1001255.

Zeissig, S., K. Murata, L. Sweet, J. Publicover, Z. Hu, A. Kaser, E. Bosse, J. Iqbal, M.M. Hussain, K. Balschun, C. Rocken, A. Arlt, R. Gunther, J. Hampe, S. Schreiber, J.L. Baron, D.B. Moody, T.J. Liang, and R.S. Blumberg. 2012. Hepatitis B virus-induced lipid alterations contribute to natural killer T cell-dependent protective immunity. *Nat. Med.* 18:1060-1068.

Figure Legends

Figure 1. IL-15 does not support RORγt$^+$ NKT cell homeostasis

(A) Spleen and liver NKT cells (α-GalCer/CD1d tetramer$^+$/ αβTCR$^+$) sub-divided by CD4 and NK1.1 by flow cytometry (left panel). Histograms depict surface expression of CD122 compared to isotype control (right panel). Red line indicates subset associated with IL-17 production. (B) Expression of CD122 on spleen, liver and pLN RORγt NKT subsets, shown as representative flow cytometry dot plots (left) and MFI (right). (C) Intracellular cytokine staining of electronically-gated NKT cells from cultures of C57BL/6 wild-type (WT) and IL-15$^{-/-}$ spleen cells. (D) RORγt$^+$ NKT cells shown as percentage of total NKT cells and absolute number from spleen and liver of WT and IL-15$^{-/-}$ mice. (E) CFSE profiles of congenically marked NKT cells recovered from livers day 7 post-transfer into sublethally irradiated WT and IL-15$^{-/-}$ mice. RORγt subsets were electronically gated, depicted with cell divisions (left), proportion RORγt$^+$ of recovered donor cells (middle) and cell recovery in IL-15$^{-/-}$ hosts as a percentage of cells recovered from WT hosts (dotted line at 100%) (right). Data are representative of two to four independent experiments with two to three mice per group per experiment. Data in (D) are means ± SEM for WT (n=13) and IL-15$^{-/-}$ (n=7) mice. Data in (E), middle and right panels, include data from 3 independent experiments with WT (n=7) and IL-15$^{-/-}$ (n=5). *, P ≤ 0.05; **, P ≤ 0.01; ***, P ≤ 0.001; ****, P ≤ 0.0001.

Figure 2. IL-7 favours the expansion of IL-17 producing NKT cells

Mice were injected intraperitoneally (i.p.) with control PBS, IL-7/IL-7 mAb (M25), IL-2/IL-2 mAb (JES6-1 or S4B6) or IL-15/IL-15RαFc (1 μg/5 μg) on days -2, -1, and 0 and analyzed as detailed below. (A) NKT cells were sorted from pooled spleens on day 3 post-*in vivo* treatment and cultured in wells coated with anti-CD3 (10 μg/ml) and anti-CD28 mAb (10 μg/ml) for 24 h. Culture supernatants were analyzed using cytokine bead array. (B) Intracellular cytokine staining of electronically-gated NKT cells from spleen cultures prepared on day 3 post-*in vivo* treatment. (C)

Proportion of RORγt^{+} cells in spleen, liver and pLN NKT cells on day 5 post-*in vivo* treatment. (D) Absolute numbers of RORγt subsets on day 5 post-*in vivo* treatment. Number above each column represents fold change compared to control. Data are representative of two to five independent experiments with two to three mice per group per experiment. Data are mean values ± SEM. *, P ≤ 0.05; **, P ≤ 0.01; ***, P ≤ 0.001 compared to control.

Figure 3. RORγt^{+} NKT cells depend exclusively on IL-7 for survival

(A) Intracellular cytokine staining of electronically-gated NKT cells from cultured WT and IL-7$^{-/-}$ spleen cells. (B) Proportion of RORγt^{+} cells in spleen, liver and thymus NKT cells from WT and IL-7$^{-/-}$ mice. (C) Absolute number of total NKT cells (upper) and RORγt^{+} NKT cells (lower) within the spleen, liver and thymus of WT and IL-7$^{-/-}$ mice. Fold change between WT and IL-7$^{-/-}$ depicted above columns. (D) CFSE profiles of congenically marked NKT cells recovered from livers on day 7 post-transfer into sublethally irradiated WT and IL-7$^{-/-}$ mice. RORγt subsets were electronically gated from recovered cells, depicted with cell divisions (left), proportion RORγt^{+} of recovered donor cells (middle) and cell recovery in IL-7$^{-/-}$ hosts as a percentage of cells recovered from WT hosts (dotted line at 100%) (right). Data are representative of two to three independent experiments with two to four mice per group per experiment. Data in (B) represent means ± SEM for WT (n=13) and IL-7$^{-/-}$ (n=6) mice. For (C) n=6 mice per group. Data in (D), middle and right panels, include data from 3 independent experiments with WT (n=7) and IL-7$^{-/-}$ (n=7). ***, P ≤ 0.001; ****, P ≤ 0.0001 compared to control.

Figure 4. The role of TCR ligation, STAT signaling and the PI3K/Akt/mTOR pathway in IL-7 mediated NKT expansion

(A) CFSE profiles of congenically marked NKT cells recovered from livers of WT and CD1d$^{-/-}$ mice one week after transfer. Mice were injected i.p. with IL-7/IL-7 mAb on days 1, 2 and 3. (B)

Intracellular phosphorylation of STAT5 and STAT3 in electronically gated NKT cell subsets from pLN after stimulation with IL-7 (10 ng/mL) (shaded histograms) or unstimulated (open histograms). (C) Intracellular phosphorylation of AKT in NKT cells sorted from pooled spleen and pLN and cultured overnight with IL-7 and Rat IgG2b isotype control or IL-7 and anti-CD1d, as measured by flow cytometry; histograms (left) and ΔMFI (right). RORγt$^+$ and RORγt$^-$ cells electronically gated for analysis. (D) Proliferation of electronically gated RORγt$^+$ NKT cells sorted from pooled spleen and pLN, as measured by CFSE dilution, after 64 h culture with IL-7 and inhibitors. Data are representative of two to three independent experiments with at least two mice per group per experiment. For (C), ΔMFI was calculated from 3 independent experiments. For (C) and (D), cells were sorted from 5-10 mice and pooled for *in vitro* culture. Data are mean values ± SEM. *, $P \leq 0.05$; **, $P \leq 0.01$ of RORγt$^+$ compared to RORγt$^-$ cells.

Figure 5. RORγt$^+$ NKT cells express low SOCS3 and high IL-7 receptor and do not convert to RORγt$^-$ in the absence of IL-7

(A) Intracellular expression of SOCS3 and SOCS1 protein compared to RORγt in NKT cells from the spleen and pLN, shown as representative flow cytometry dot plots (left) and MFI (right). (B) Socs1 and Socs3 mRNA expression of NKT subsets as evaluated by real time PCR, normalised to Gapdh. Fold change of NK1.1$^-$CCR6$^+$CD103$^+$ subset relative to NK1.1$^+$CCR6$^-$CD103$^-$ subset. (C) Expression of IL-7Rα on spleen, liver and pLN RORγt NKT subsets, shown as representative flow cytometry dot plots (left) and MFI (right). (D) Expression of IL-7Rα on memory phenotype (MP) and naïve CD8$^+$ T cells, RORγt$^-$ and RORγt$^+$ NKT cells from pLN. (E) In vitro proliferation of electronically gated NKT cells from spleen and liver as measured by CFSE dilution, after 72 h culture with IL-7. Proportion of divided cells shown. (F) Proliferation of purified IL-7Rα intermediate-high and low expressors as measured by CFSE dilution after 72 h culture with IL-7. RORγt was electronically gated upon analysis. (G) Sorted RORγt-GFP^{neg} NKT cells analysed for proliferation using CTV one week after transfer into congenic hosts injected with IL-7/IL-7 mAb on

days 1-5. Percentage GFP^+ donor cells depicted in column graph. (H) RORγt expression of sorted RORγt-GFP^{pos} NKT cells recovered from livers on day 8 post-transfer into sublethally irradiated WT and IL-$7^{-/-}$ mice. Cell recovery in IL-$7^{-/-}$ hosts as a percentage of cells recovered from WT hosts (dotted line at 100%) depicted in column graph. Data are representative of two to four independent experiments with at least two mice per group per experiment. Data in (A) represent means ± SEM with n=5 mice per group, representative of four experiments. *, $P \leq 0.05$; **, $P \leq 0.01$; ***, $P \leq 0.001$. For (B, F-H), cells were sorted from 5-10 mice and pooled for experiments.

Supplementary Figure Legends

Supplementary Figure 1. IL-7 favours the expansion of $CD4^-NK1.1^-$ NKT cells

Mice were injected intraperitoneally (i.p.) with control PBS or IL-7/IL-7 mAb (M25) (1 μg/5 μg) on days -2, -1, and 0 and analyzed on day 5. NKT cells were electronically gated and analysed as a percentage of spleen and liver lymphocytes and absolute numbers (upper panels). NKT cells were analyzed for subset composition using CD4 and NK1.1 (lower panels). Number above each column represents fold change of that subset compared to control. Data are representative of two to three independent experiments with two to three mice per group per experiment. Data are mean values ± SEM.

Supplementary Figure 2. IL-7 favours the expansion of $CD4^-$ RORγt^+ NKT cells

(A) Spleen, liver and peripheral lymph node (pLN) NKT cells (α-GalCer/CD1d $tetramer^+$/ $\alpha\beta TCR^+$) were electronically gated and analysed by flow cytometry for the expression of surface CD4, NK1.1 and intracellular RORγt. (B) Intracellular cytokine staining of electronically-gated NKT cells from spleen cultures prepared on day 3 post-*in vivo* treatment with IL-7/IL-7 mAb.

Proportion CD4-positive and -negative cells within IL-17 producing NKT cells shown (lower panel). (C) CD4-positive and -negative RORγt^{+} NKT cells shown as proportion (left panel) and absolute number (right panel) in the spleen of control and IL-7/IL-7 mAb treated mice on day 5 post-*in vivo* treatment. Number above each column represents fold change compared to control. Data are representative of three independent experiments with two to three mice per group per experiment. Data are mean values ± SEM. **, P ≤ 0.01.

Supplementary Figure 3. Phosphorylation of STAT5 in NKT cells after IL-7 stimulation

Intracellular phosphorylation of STAT5 in electronically gated NKT cell subsets from peripheral lymph nodes after stimulation with different concentrations of IL-7. Shaded histograms depict IL-7-stimulated cells and open histograms depict unstimulated controls.

Supplementary Figure 4. Isolation of RORγt NKT subsets

(A) Proportion RORγt-positive or RORγt-negative cells of spleen and lymph node tetramer^{+}NK1.1^{-} CCR6^{+}CD103^{+} and tetramer^{+}NK1.1^{+}CCR6^{-}CD103^{-} subsets that were used to represent RORγt subsets in Figure 5B. (B) Illustration of a post-sort analysis of peripheral LN and spleen cells sorted into Tet^{+}NK1.1^{-}CCR6^{+}CD103^{+} and Tet^{+}NK1.1^{+}CCR6^{-}CD103^{-} subsets, representative of RORγt^{+} and RORγt^{-} subsets respectively for Figure 5B. (C) Separation of splenic NKT cells into IL-7Rα intermediate-high and low expressors by cell sorting. (D) Separation of splenic RORγt-GFP^{neg} NKT cells and RORγt-GFP^{pos} NKT cells from Rorc(γt)^{GFP} mice.

Supplementary Figure 5. Expression of IL-7Rα on NKT cells subsets

Spleen and liver NKT cells (α-GalCer/CD1d tetramer^{+}/ αβTCR^{+}) were divided into subsets using CD4 and NK1.1 by flow cytometry. Histograms depict the surface expression of IL-7Rα (CD127) for each subset as indicated, compared to isotype control. Red line indicates the subset associated with IL-17 production.

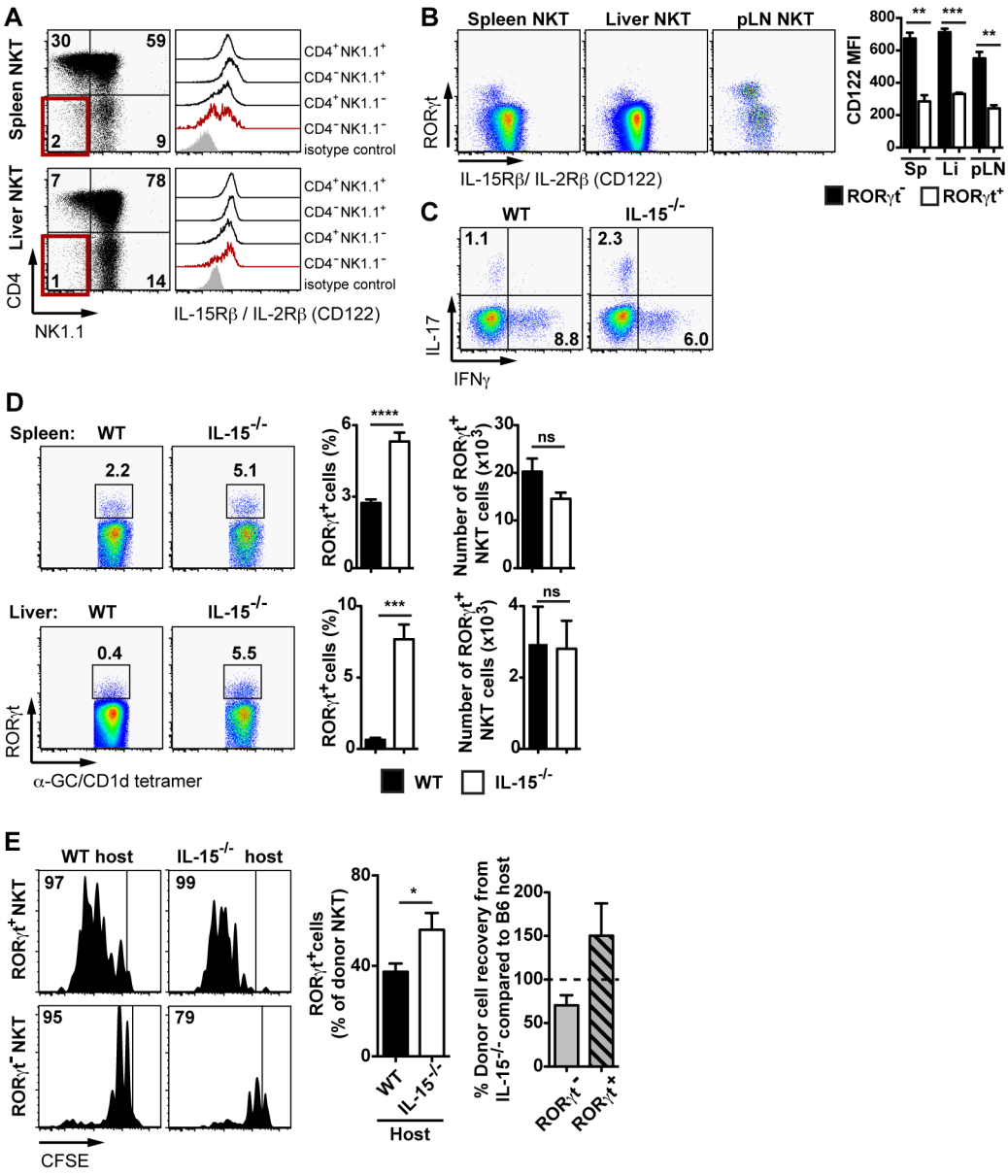

Webster *et. al.* Figure 1

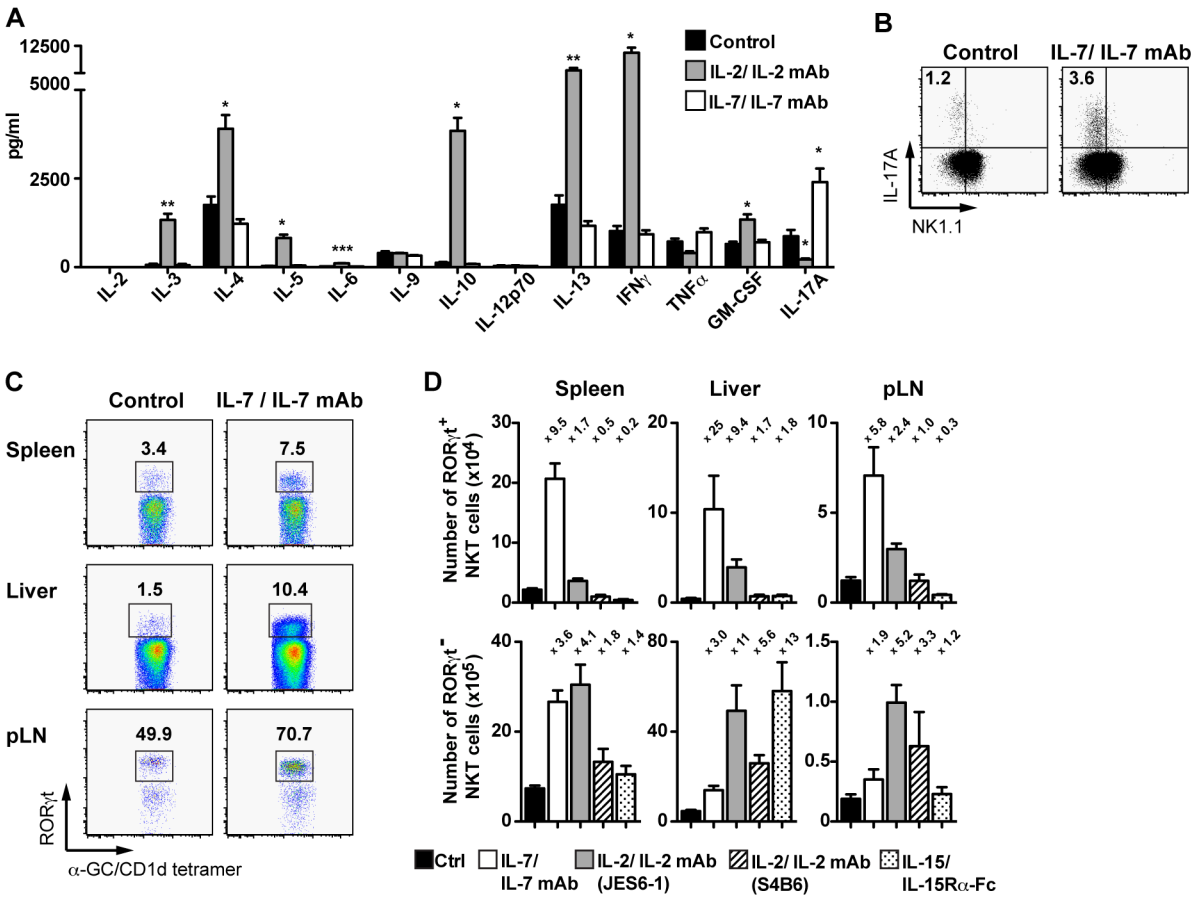

Webster *et. al.* Figure 2

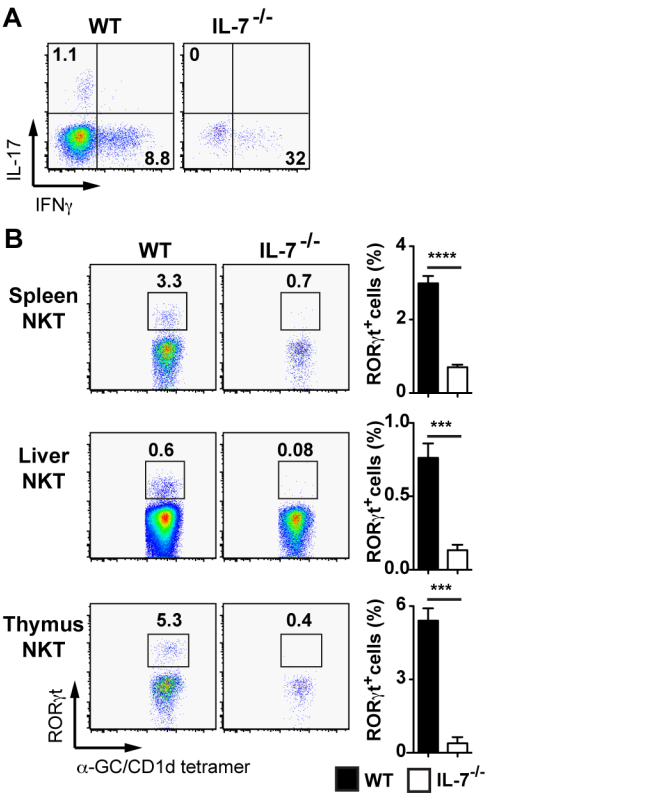

Webster *et. al.* Figure 3

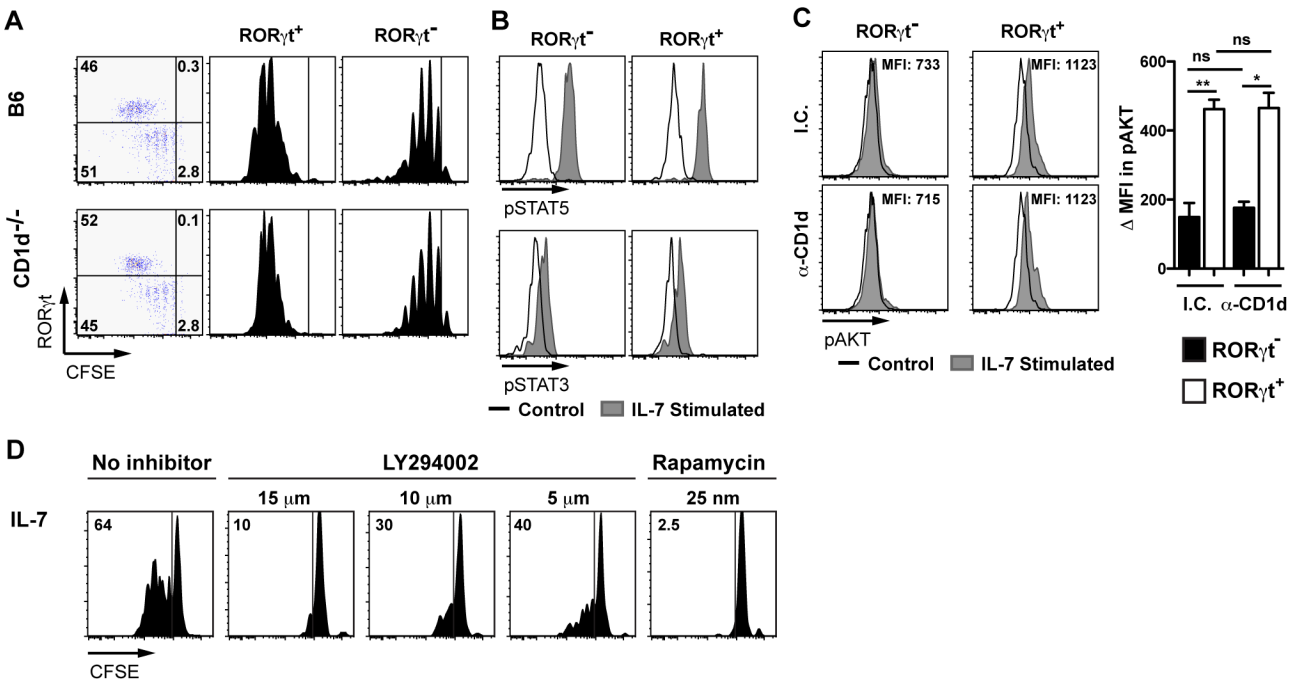

Webster *et. al.* Figure 4

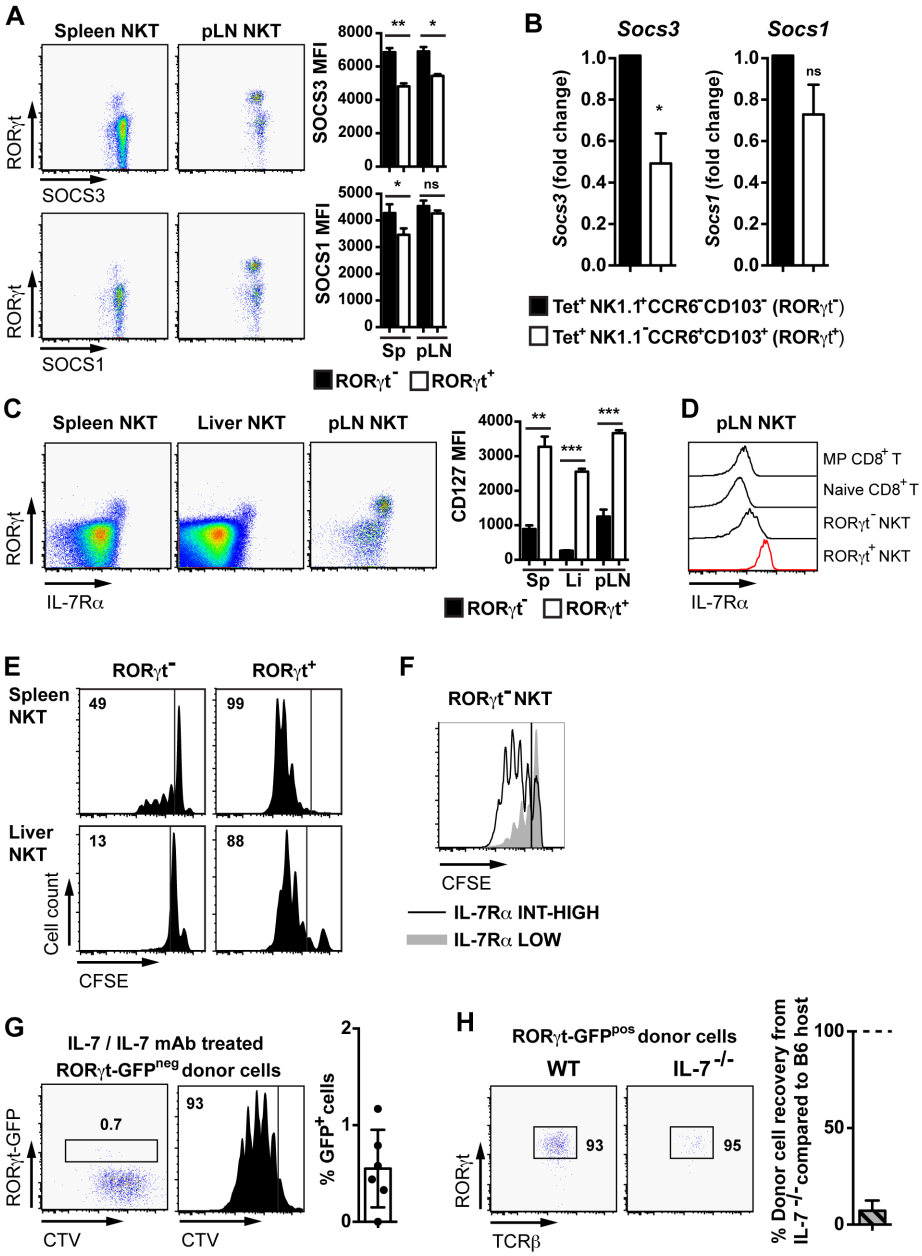

Webster *et. al.* Figure 5

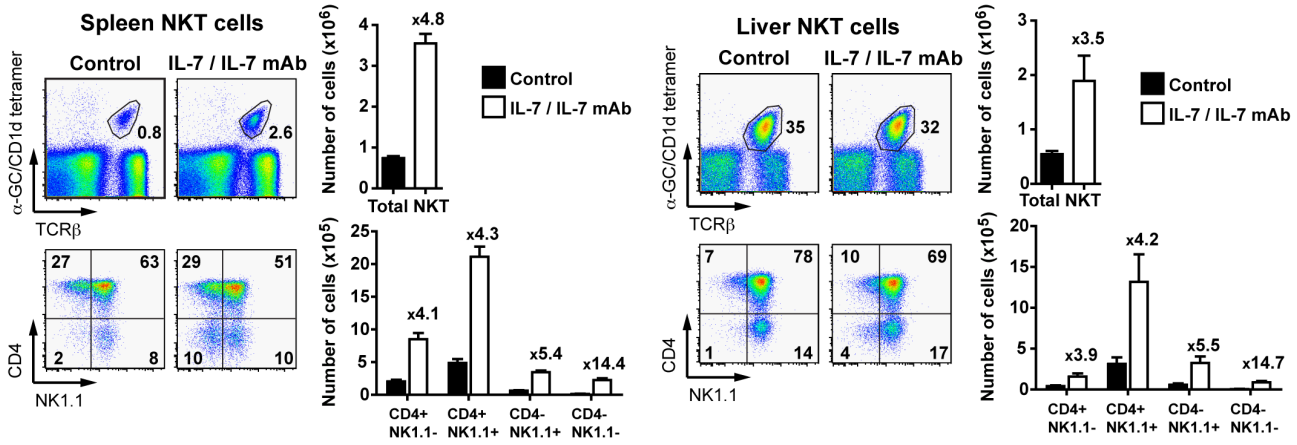

Webster *et. al.* Supplementary Figure 1

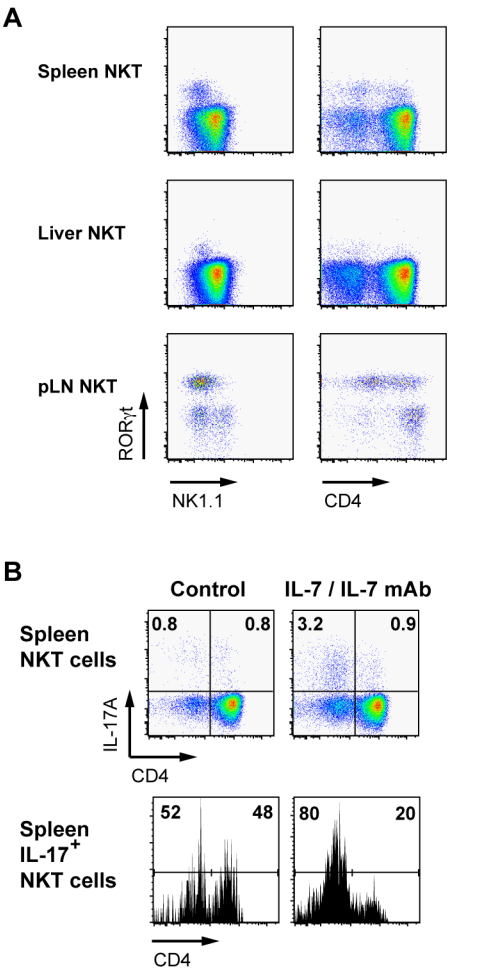

Webster *et. al.* Supplementary Figure 2

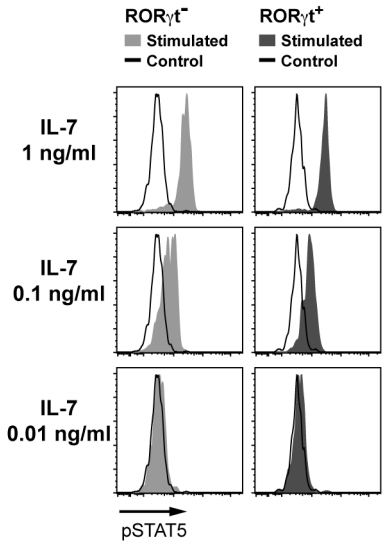

Webster *et. al.* Supplementary Figure 3

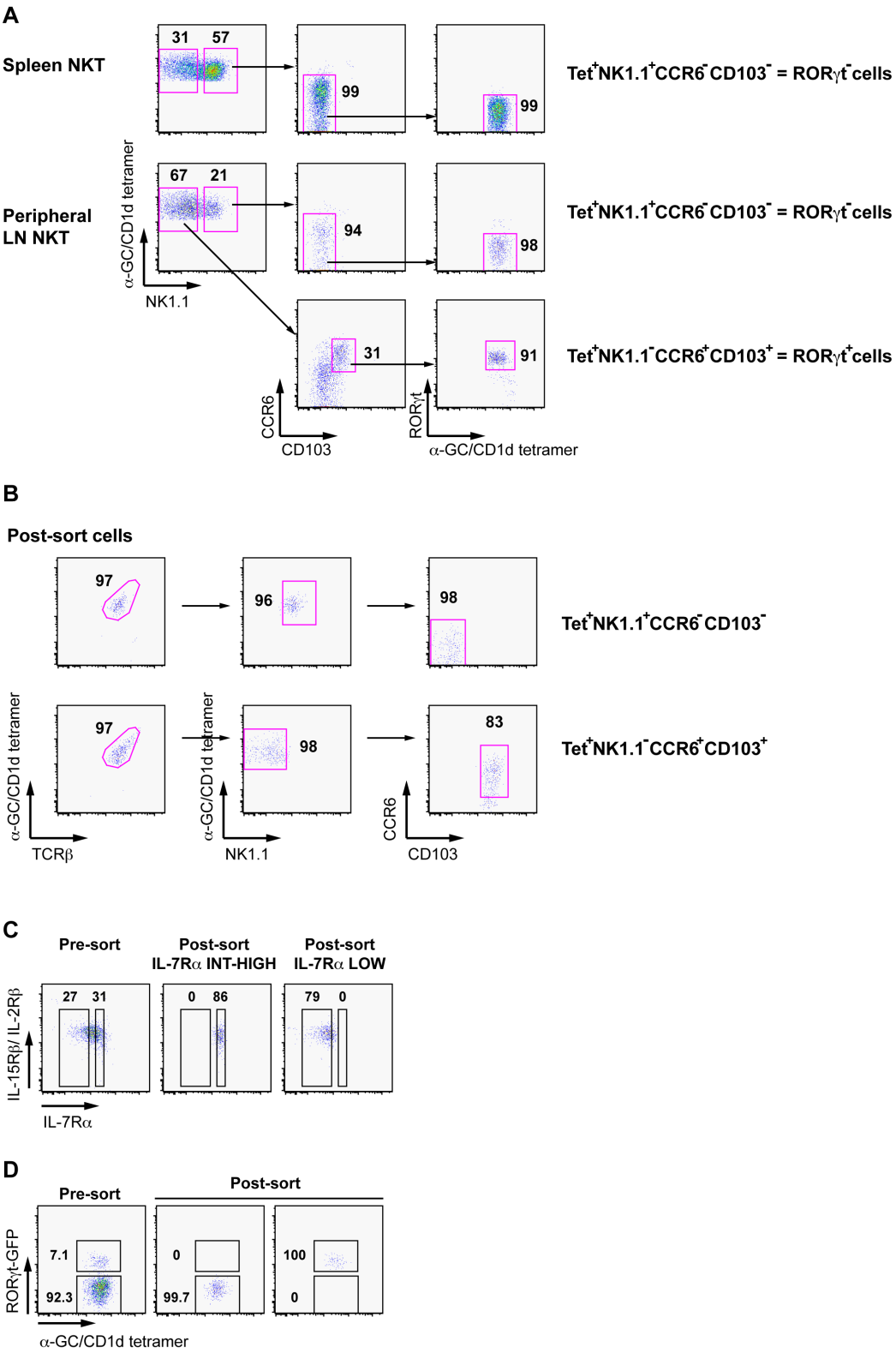

Webster *et. al.* Supplementary Figure 4

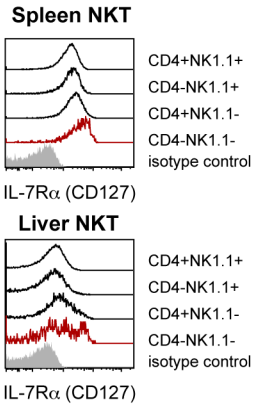

Webster *et. al.* Supplementary Figure 5